Inorg. Chem. **2008**, *47*, 6051−6055

Crystal Structure and Chemical Bonding of Mg_3Ru_2

Rainer Pöttgen,*,† Viktor Hlukhyy,‡ Aleksey Baranov,§ and Yuri Grin§

Institut für Anorganische und Analytische Chemie, Universität Münster, Corrensstrasse 30, 48149 Münster, Germany, Department Chemie, TU München, Lichtenbergstraβe 4, 85747 Garching, Germany, and Max-Plank-Institut für Chemische Physik fester Stoffe, Nöthnitzer Straβe 40, 01187 Dresden, Germany

Received February 29, 2008

Mg_3Ru_2 was prepared by a reaction between the elements in the ideal ratio in a sealed tantalum ampule. Its β-manganese type crystal structure was refined on the basis of the single-crystal data: space group $P4_132$, a = 693.52(6) pm, wR2 = 0.024, 168 F^2 values, and 10 parameters. The magnesium (CN = 14) and ruthenium (CN = 12) atoms are completely ordered on the 12d and 8c sites of the crystal structure of β-manganese. Both environments can be considered as Frank−Kasper related polyhedra. A periodic nodal surface $P4_132\langle(110)^1_\pi\rangle P4_132$ separates the magnesium and ruthenium positions in two different labyrinths, suggesting different chemical interactions within different parts of the structural motif. Analysis of the chemical bonding with the electron localizability indicator (ELI-D) reveals covalently interacting three-bonded ruthenium atoms, forming a 3D network. The network interacts with the magnesium substructure by multicenter bonds.

Introduction

The binary-phase diagram magnesium−ruthenium has been investigated by Westin and Edshammar.[1] They reported the cubic intermetallic compounds Mg_3Ru_2 with a β-manganese structure and $Mg_{6.2}Ru$ with $Mg_{44}Rh_7$ type. Both phases have been investigated via X-ray powder and single crystal film data using the Guinier−Hägg and Weissenberg techniques.

The crystal structure of $Mg_{6.2}Ru$ contains three ruthenium and eleven magnesium positions. Two of these positions show Ru/Mg mixing, indicating a small homogeneity range for this compound.

The refinement of the Mg_3Ru_2 structure led only to a residual of R = 0.17 and the authors themselves suggested a further careful single-crystal study. In the course of our systematic studies of binary and pseudobinary transition-metal−magnesium compounds,[2−10] we have prepared a new sample of Mg_3Ru_2. A precise structure refinement and a detailed analysis of chemical bonding are reported herein.

Experimental Section

Synthesis. Starting materials for the preparation of Mg_3Ru_2 were a magnesium rod (Johnson Matthey, Ø = 16 mm, >99.5%) and ruthenium powder (Degussa-Hüls, ca. 200 mesh, >99.9%). Pieces of the magnesium rod (the surface of the rod was first cut on a turning lathe to remove surface impurities) and the ruthenium powder were weighed in the ideal 3:2 atomic ratio and sealed in a small tantalum tube (ca. 1 cm^3 tube volume) under an argon pressure of ca. 800 mbar.[11] The argon was purified before over molecular sieves, silica gel, and titanium sponge (900 K).

The tantalum tube was then placed in a water-cooled sample chamber[12] of a high-frequency furnace (Hüttinger Elektronik, Freiburg, Typ TIG 2.5/300), rapidly heated at 1350 K, kept at that temperature for one hour, and then slowly cooled to room

* To whom correspondence should be addressed. E-mail: pottgen@uni-muenster.de (R.P.), viktor.hlukhyy@lrz.tum.de (V.H.), grin@cpfs.mpg.de (Y.G.), baranov@cpfs.mpg.de (A.B.).
† Universität Münster.
‡ TU München.
§ Max-Plank-Institut für Chemische Physik fester Stoffe.

(1) Westin, L.; Edshammar, L.-E. *Chem. Scr.* **1973**, *3*, 15–22.
(2) Hlukhyy, V.; Hoffmann, R.-D.; Pöttgen, R. *Z. Anorg. Allg. Chem.* **2004**, *630*, 68–74.
(3) Hlukhyy, V.; Hoffmann, R.-D.; Pöttgen, R. *Intermetallics* **2004**, *12*, 383–387.
(4) Hlukhyy, V.; Pöttgen, R. *J. Solid State Chem.* **2004**, *177*, 1646–1650.
(5) Hlukhyy, V.; Pöttgen, R. *Intermetallics* **2004**, *12*, 533–537.
(6) Hlukhyy, V.; Rodewald, U. Ch.; Hoffmann, R.-D.; Pöttgen, R. *Z. Naturforsch.* **2004**, *59b*, 251–255.
(7) Černý, R.; Renaudin, G.; Favre-Nicolin, V.; Hlukhyy, V.; Pöttgen, R. *Acta Crystallogr. B* **2004**, *60*, 272–281.
(8) Hlukhyy, V.; Pöttgen, R. *Solid State Sci.* **2004**, *6*, 1175–1180.
(9) Hlukhyy, V.; Pöttgen, R. *Z. Naturforsch.* **2004**, *59b*, 943–946.
(10) Hlukhyy, V.; Pöttgen, R. *J. Solid State Chem.* **2005**, *178*, 79–84.
(11) Pöttgen, R.; Gulden, Th.; Simon, A. *GIT Labor-Fachzeitschrift* **1999**, *43*, 133–136.
(12) Kuβmann, D.; Hoffmann, R.-D.; Pöttgen, R. *Z. Anorg. Allg. Chem.* **1998**, *624*, 1727–1735.

10.1021/ic800387a CCC: $40.75
Published on Web 06/12/2008

Table 1. Crystallographic Data and Structure Refinement for Mg_3Ru_2

empirical formula	Mg_3Ru_2
fw	275.07 g/mol
unit cell dimensions	$a = 693.52(6)$ pm
(powder diffraction data)	$V = 0.3336$ nm^3
Pearson symbol	*cP*20
structure type	*β*-Mn
space group	$P4_132$
formula units per cell	$Z = 4$
calculated density	5.48 g/cm^3
transmission ratio (max/min)	0.574: 0.543
absorption coefficient	9.3 mm^{-1}
F (000)	496
θ range for data collection	4° to 30°
ranges in h, k, l	±9, ± 9, ± 9
total no. of reflns	3844
independent reflns	168 ($R_{int} = 0.074$)
reflns with $I > 2\sigma(I)$	153 ($R_{sigma} = 0.019$)
data/params	168/10
GOF on F^2	1.132
final residuals [$I > 2\sigma(I)$]	R1 = 0.013; wR2 = 0.023
final residuals (all data)	R1 = 0.019; wR2 = 0.024
extinction coefficient	0.0070(9)
Flack parameter	−0.16(13)
largest diff. peak and hole	0.38 and −0.39 e/Å^3

temperature within another hour. The temperature was controlled through a Sensor Therm Metis MS09 pyrometer with an accuracy of ±20 K. The brittle product could easily be separated from the tantalum tube. No reaction with the container material was observed. The compact light-gray pieces and the dark-gray powder are stable in air over months.

X-ray powder data. The purity of the sample was checked by X-ray powder diffraction in a Guinier camera using Cu Kα_1 radiation ($\lambda = 154.056$ pm) and α-quartz ($a = 491.30$, $c = 540.46$ pm) as an internal standard. The Guinier camera was equipped with an image plate system (Fujifilm, BAS-1800). The lattice parameter (Table 1) was obtained by a least-squares refinement of the powder diffraction data. The correct indexing of the diffraction lines was ensured through an intensity calculation[13] using the positional parameters of the refined crystal structure. The obtained value is in good agreement with the value of 692.9 pm reported previously.[1]

Single-Crystal Data. Small single crystals of Mg_3Ru_2 were isolated from the crushed sample after the annealing procedure. The crystals were first examined on a Buerger precession camera (equipped with an image plate system, Fujifilm, BAS-1800) to establish their suitability for intensity data collection. Single-crystal intensity data were collected at room temperature by use of a four-circle diffractometer (CAD4) with graphite monochromatized Mo Kα (71.073 pm) radiation and a scintillation counter with pulse-height discrimination. Scans were taken in the $\omega/2\theta$ mode. An empirical absorption correction was applied on the basis of Ψ-scan data, followed by a spherical absorption correction. All relevant crystallographic data for the data collection and evaluation are listed in Table 1.

EDX Analyses. The composition of the single crystal investigated on the four-circle diffractometer was analyzed using a LEICA 420 I scanning electron microscope with MgO and elemental ruthenium as standards. No impurity elements heavier than sodium were observed. The composition determined by EDX (60 ± 1 at.-% Mg; 40 ± 1 at.-% Ru) was in good agreement with the results of the crystal-structure determination (Mg_3Ru_2).

Computational Details. Electronic structure calculation and bonding analysis were carried out using the TB-LMTO-ASA program package.[14] The Barth−Hedin exchange potential[15] was employed for the LDA calculations. The radial scalar-relativistic Dirac equation was solved to get the partial waves. Although the calculation within the atomic sphere approximation (ASA) includes corrections for the neglect of interstitial regions and partial waves of higher order,[16] an addition of empty spheres was not necessary. The following radii of the atomic spheres were applied for the calculations: r(Mg) = 1.656 Å, r(Ru) = 1.465 Å. A basis set containing Mg(3s,3p) and Ru(5s,5p,4d) orbitals was employed for a self-consistent calculation with Mg(3d) and Ru(4f) functions being downfolded.

To investigate the stability of the calculation results with respect to the calculation method, additional calculations of the electronic structure of Mg_3Ru_2 were performed with the FPLO code[17] utilizing a minimal basis set of numerical local orbitals. The Perdew−Wang exchange-correlation potential[18] was employed for the scalar-relativistic calculation. Mg(3s,3p,3d) and Ru(5s,5p,5d) states were treated as valence states, whereas Mg(2s,2p) and Ru(4s,4p) were treated as semi-core states. Lower-lying core states were treated fully relativistically. A mesh of 94 irreducible k points was used.

The electron localizability indicator (ELI, Y) was evaluated according to ref 19 with an ELI module implemented within the *TB-LMTO-ASA*[14] and *FPLO*[20] program packages. The topology of ELI was analyzed using the program *Basin*[21] with consecutive integration of the electron density in basins, which are bound by zero-flux surfaces in the ELF gradient field. This procedure, similar to the one proposed by Bader for the electron density,[22] allows us to assign an electron count for each basin, revealing additional information about the chemical bonding.

Results and Discussion

Structure Refinement. The atomic positions of Mg_3Ru_2 from ref 1 were taken as starting values, and the structure was refined using *SHELXL-97* (full-matrix least-squares on F^2)[23] with anisotropic atomic displacement parameters for all atoms. Because the work on $Mg_{6.2}Ru$[1] revealed Ru/Mg mixing for two positions, the occupancy parameters of Mg_3Ru_2 were refined in a separate series of least-squares cycles to check for a possible deviation from the ideal composition. Both sites were fully occupied within less than one standard uncertainty, and in the final cycles the ideal occupancy parameters were assumed. Refinement of the correct absolute structure ($P4_132$ vs $P4_332$) was ensured through calculation of the Flack parameter.[24,25] A final difference electron-density map did not reveal any significant residual peaks. The results of the structure refinement are

(13) Yvon, K.; Jeitschko, W.; Parthé, E. *J. Appl. Crystallogr.* **1977**, *10*, 73–74.
(14) Jepsen, O.; Burkhardt, A.; Andersen, O. K. *The Program TB-LMTO-ASA, ver. 4.7; Max-Planck-Institut für Festkörperforschung: Stuttgart,* 1999.
(15) Barth, U.; Hedin, L. *J. Phys. C* **1972**, *5*, 1629–1642.
(16) Andersen, O. K. *Phys. Rev. B* **1975**, *12*, 3060–3083.
(17) Koepernik, K.; Eschrig, H. *Phys. Rev. B* **1999**, *59*, 1743–1757.
(18) Perdew, J. P.; Wang, Y. *Phys. Rev. B* **1992**, *45*, 13244–13249.
(19) Kohout, M. *Int. J. Quantum Chem.* **2004**, *97*, 651–658.
(20) Ormeci, A.; Rosner, H.; Wagner, F. R.; Kohout, M.; Grin, Yu. *J. Phys. Chem. A* **2006**, *110*, 1100–1105.
(21) Kohout, M. *Basin. Version 4.1*; Max-Planck-Institut für Chemische Physik fester Stoffe: Dresden, 2006.
(22) Bader, R. F. W. *Atoms in Molecules: A Quantum Theory*; Oxford University Press: Oxford, 1999.
(23) Sheldrick, G. M. *SHELXL-97, Program for Crystal Structure Refinement*; University of Göttingen: Germany, 1997.
(24) Flack, H. D.; Bernadinelli, G. *Acta Crystallogr.* **1999**, *55A*, 908–915.
(25) Flack, H. D.; Bernadinelli, G. *J. Appl. Crystallogr.* **2000**, *33*, 1143–1148.

Table 2. Atomic Coordinates and Isotropic Displacement Parameters (pm^2) for Mg_3Ru_2[a]

atom	site	*x*	*y*	*z*	U_{eq}
Mg	12d	1/8	0.2051(1)	$y + 1/4$	79(3)
Ru	8c	0.07378(3)	*x*	*x*	54(1)

[a] U_{eq} is defined as one third of the trace of the orthogonalized U_{ij} tensor.

Table 3. Interatomic Distances (pm) of Mg_3Ru_2 (Standard Deviations in Parentheses)

Mg:	2	Ru	282.0(1)	Ru:	3	Ru	255.3(1)
	2	Mg	288.6(2)		3	Mg	282.0(1)
	2	Ru	291.2(1)		3	Mg	291.2(1)
	4	Mg	292.5(1)		3	Mg	296.4(1)
	2	Ru	296.4(1)				
	2	Mg	357.8(1)				

summarized in Table 1. The atomic coordinates and the interatomic distances are listed in Tables 2 and 3. Further information on the structure refinement is available.[44]

Crystal Chemistry. Mg_3Ru_2 crystallizes with an ordered version of the β-manganese structure with magnesium on the 12d and ruthenium on the 8c site. The present refinement is considerably more precise than the previous refinement based on Weissenberg diffraction data registered on film.[1] Also we clearly rule out ruthenium−magnesium mixing.

The larger magnesium atoms have a coordination number of 14 with 6 ruthenium and 8 magnesium neighbors in the form of a Frank−Kasper related polyhedron,[2628] however, Mg_3Ru_2 cannot be considered as a true Frank−Kasper phase. The ruthenium atoms have 12 neighbors (3Ru + 9Mg) in distorted icosahedral coordination (Figure 1). The Ru−Mg distances in Mg_3Ru_2 range from 282 to 296 pm and are slightly larger than the sum of the covalent radii of 260 pm.[28] In the $Mg_{44}Rh_7$-type structure of $Mg_{6.2}Ru$,[1] the Ru−Mg distances in the three $RuMg_{12}$ icosahedra range from 262 to 315 pm with an average value of 290 pm.

Whereas no Ru−Ru contacts occur in the magnesium-rich structure of $Mg_{6.2}Ru$, each ruthenium atom in Mg_3Ru_2 has three ruthenium neighbors at the remarkably short Ru−Ru distance of 255 pm, much smaller than the average Ru−Ru distance of 268 pm in *hcp* ruthenium.[29] Also, in various organometallic ruthenium cluster compounds the Ru−Ru distances are longer than 280 pm.[30–32] This is also the case for $Bi_{24}Ru_3Br_{20}$,[33] Bi_4RuBr_2, and Bi_4RuI_2.[34]

At this point it is worthwhile to note that the ruthenium substructure of Mg_3Ru_2 is isopointal with the silicide substructure of the Zintl phase $SrSi_2$,[35] nicely underlining the anionic nature of ruthenium. The PES descriptors for $SrSi_2$ have recently been reported by Leoni and Nesper.[36]

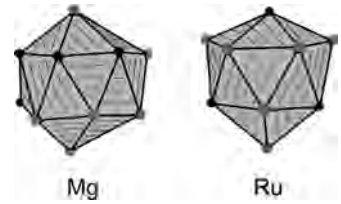

Figure 1. Coordination polyhedra in the crystal structure of Mg_3Ru_2: (a) $Mg[Ru_6Mg_8]$; (b) $Ru[Ru_3Mg_9]$. Magnesium and ruthenium atoms are shown as black and medium-gray circles, respectively.

The Mg−Mg distances cover the wide range from 289 to 358 pm. The shorter ones are even shorter than the average Mg−Mg distance of 320 pm in *hcp* magnesium.[20] The two magnesium atoms at the longest Mg−Mg distance of 358 pm still belong to the magnesium coordination sphere. Similar wide ranges of Mg−Mg distances are observed in the structures of Mg_5Pd_2,[5] Mg_3Rh, $Mg_{13}Ir_3$,[6] or MgIr.[7]

The two crystallographically independent manganese atoms in the β-manganese structure have longer (257 pm) Mn−Mn distances for 12d and shorter (236 pm) for the 8c manganese atoms. Nesper assumed that the majority component might have cationic and the minority component anionic character.[37] Following this assumption, magnesium with the smaller Pauling electronegativity (1.31) should occupy the cationic 12d site in the crystal structure of Mg_3Ru_2, whereas the more electronegative ruthenium atoms (2.20 on the Pauling scale[28]) would fill the anionic 8c positions.

Chemical Bonding Analysis. Periodic nodal surfaces (PNS) were shown to be an appropriate tool to detect different atomic interactions in crystal structures.[38,39] Especially in the structures of intermetallic compounds, PNS separate regions with different bonding types: covalent from van der Waals bonds in $RhBi_4$[40] and $PdGa_5$,[41] two-center from three-center bonds in $CuAl_2$,[42] or covalent from ionic bonds in clathrates.[43] Indeed, the appropriate PNS $P4_132\langle(110)\frac{1}{\pi}\rangle P4_132$ (notation according to 41) separates the magnesium and ruthenium positions in two different labyrinths (part a of Figure 2). Ruthenium atoms are located in the brown labyrinth and vertices-condensed magnesium octahedra are found in the beige labyrinth, suggesting different interactions within and between the labyrinths. To shed more light on the atomic interactions in Mg_3Ru_2, analysis of chemical bonding in real space was performed, applying a electron localizability indicator (ELI-D).

(26) Frank, F. C.; Kasper, J. S. *Acta Crystallogr.* **1958**, *11*, 184–190.
(27) Frank, F. C.; Kasper, J. S. *Acta Crystallogr.* **1959**, *12*, 483–499.
(28) Emsley, J. *The Elements*; Clarendon Press: Oxford, 1989.
(29) Donohue, J. *The Structures of the Elements*; Wiley: New York, 1974.
(30) Adams, R. D.; Captain, B.; Pellechia, P. J.; Zhu, L. *Inorg. Chem.* **2004**, *43*, 7243–7249.
(31) Zhong, X.; Ang, S.-G.; Ang, H.-G. *J. Organomet. Chem.* **2004**, *689*, 361–368.
(32) Wunder, M.; Rauchfuss, T. B.; Fenske, D. *Z. Anorg. Allg. Chem.* **2004**, *630*, 1578–1580.
(33) Ruck, M. *Z. Anorg. Allg. Chem.* **1997**, *623*, 1591–1598.
(34) Ruck, M. *Z. Anorg. Allg. Chem.* **1997**, *623*, 1583–1590.
(35) Janzon, K.; Schäfer, H.; Weiss, A. *Angew. Chem.* **1965**, *77*, 258–259.
(36) Leoni, S.; Nesper, R. *Solid State Sci.* **2003**, *5*, 95–107.
(37) Nesper, R. *Angew. Chem.* **1991**, *103*, 805–834.
(38) von Schnering, H. G.; Nesper, R. *Z. Phys. B: Condens. Matter* **1991**, *83*, 407–412.
(39) von Schnering, H. G.; Nesper, R. *Angew. Chem., Int. Ed. Engl.* **1987**, *26*, 1059–1080.
(40) Grin, Yu.; Wedig, U.; von Schnering, H. G. *Angew. Chem., Int. Ed. Engl.* **1995**, *34*, 1204–1206.
(41) Grin, Yu.; Wedig, U.; Wagner, F.; von Schnering, H. G.; Savin, A. *J. Alloys Compd.* **1997**, *255*, 203–208.
(42) Grin, Yu.; Wagner, F. R.; Armbrüster, M.; Kohout, M.; Leithe-Jasper, A.; Schwarz, U.; Wedig, U.; von Schnering, H. G. *J. Solid State Chem.* **2006**, *179*, 1707–1719.
(43) von Schnering, H. G.; Zürn, A.; Chang, J.-H.; Baitinger, M.; Grin, Yu. *Z. Anorg. Allg. Chem.* **2007**, *638*, 1147–1153.
(44) Details may be obtained from: Fachinformationszentrum Karlsruhe, D-76344 Eggenstein-Leopoldshafen (Germany), by quoting the Registry No. CSD-419238.

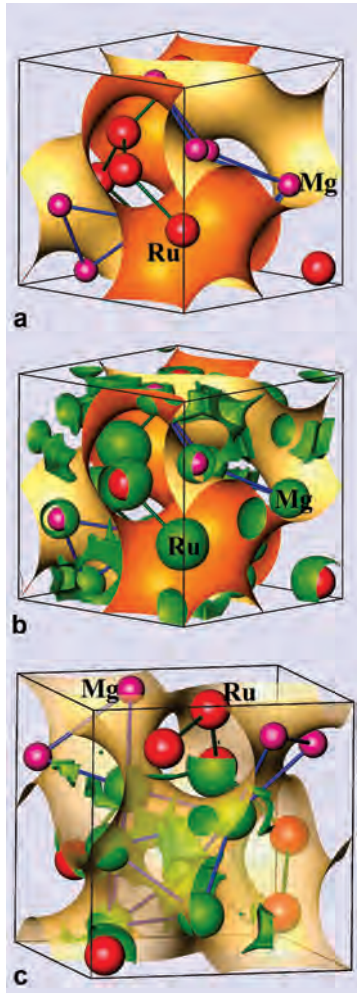

Figure 2. (a) A periodic nodal surface $P4_132\langle(110)\frac{1}{\pi}\rangle P4_132$ separates magnesium (pink) and ruthenium (red) positions in the crystal structure of Mg_3Ru_2 in two different labyrinths; (b) both labyrinths contain the inner shell attractors of ELI-D shown by the isosurface (green); (c) the bonding attractors in the vicinity of the magnesium atoms are positioned in one (beige) labyrinth.

The analysis of the ELI-D calculated with both methods mentioned above (LMTO and FPLO) shows similar topology of the functional. For comparison reasons with the previous investigations, we present hereafter the LMTO results.

The electron localizability indicator in the crystal structure of Mg_3Ru_2 shows maxima in the regions of the inner shells of the atoms and in the valence regions. In general, the distribution of the attractors follows the space separation given by the PNS (parts b and c of Figure 2): inner-shell attractors of ruthenium and bonding attractors between ruthenium atoms are located in one labyrinth (brown), the inner-shell attractors of magnesium and the bonding attractors in their vicinity are positioned in the another (beige) labyrinth of the PNS. This is in agreement with the previous tendencies,[40,43] suggesting a spatial separation of different chemical interactions and formation of the polyanionic and polycationic parts of the structure. However, detailed analysis below reveals a more complex bonding behavior.

Only slight deviations from the spherical ELI-D distribution in the vicinity of the ruthenium position are observed. Four shells can be found around each ruthenium nucleus.

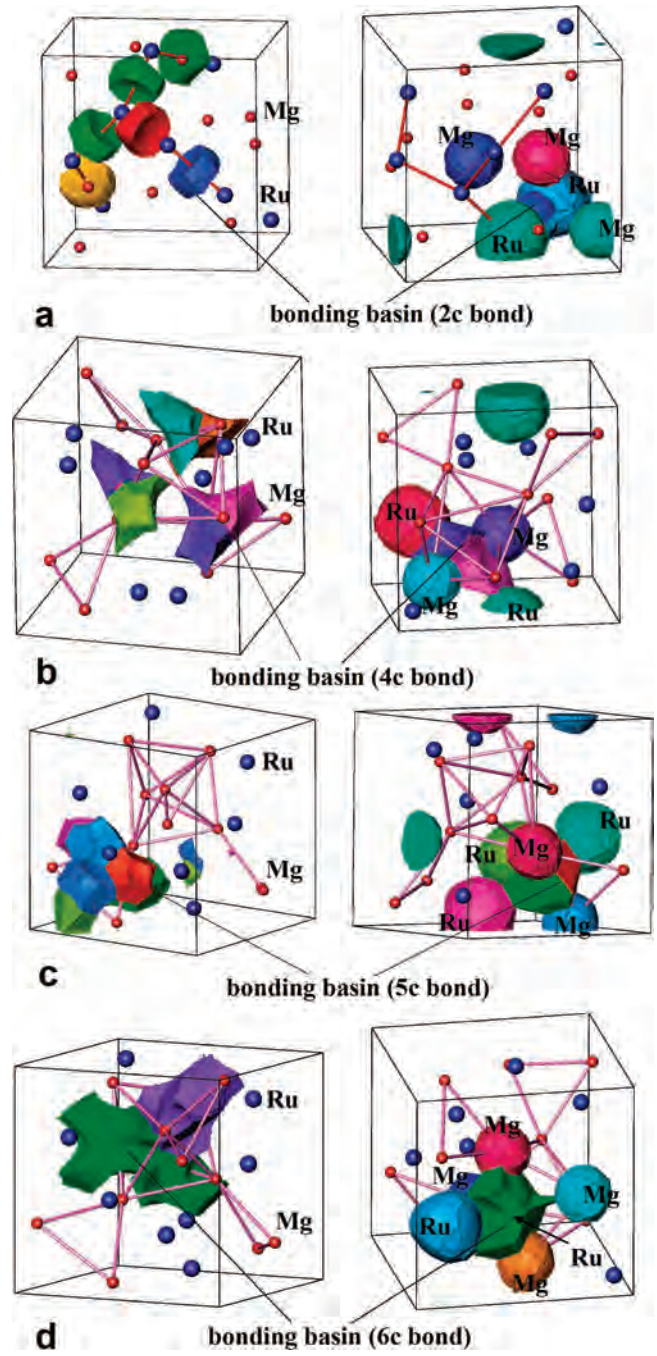

Figure 3. Four types of atomic interactions in Mg_3Ru_2 in the ELI-D representation: (left) position of the bonding basins in the crystal structure, (right) coordination of the bonding basins by the atomic core basins (synapticity of the basins). Mg−Mg contacts are shown in light pink, Ru−Ru bonds are given in red. Bonding attractors in b and c are shown as two-colored.

The fifth shell present in the isolated atom is not observed in Mg_3Ru_2. A similar spherical distribution of ELI-D is found for the inner shell of the magnesium atoms.

There are four different types of ELI-D attractors in the valence regions of the crystal structure of Mg_3Ru_2. Between the ruthenium atoms in the brown labyrinth, additional attractors were found on the Ru−Ru contacts (part a of Figure 3, left). The basin of this attractor has common surfaces merely with the core basins of the ruthenium atoms, and the core basins of the nearest magnesium atoms are

clearly separated from the Ru−Ru bonding basin (part b of Figure 3, right). This constellation reflects a two-center bonding. Integration of the electron density within the basin yields a population of 0.66 electrons.

Three other types of attractors are located closer to the magnesium atoms. The attractors on the shortest Mg−Mg contacts (288.6 pm) are shown in part b of Figure 3, left. The basin of each attractor has a population of 0.56 electrons and common surfaces with two magnesium core basins and two ruthenium core basins (part b of Figure 3, right), thus revealing the four-center interaction despite the position of the attractor between the magnesium atoms. The next attractor (part c of Figure 3, left) is positioned close to the Mg−Mg contact with a distance of 292.5 pm. Integration of the electron density gives the value of 0.73 for the population. The synapticity (i.e., the number of the core basins having common surface with the bonding basin) of its basin is five, it contacts with two core basins of magnesium and three core basins of ruthenium, representing a five-center interaction (part c of Figure 3, right). The last attractor type is located close to the longest Mg−Mg contact (357.8 pm, part d of Figure 3, left). Its population is the largest one (0.97 electrons). The shape is very complex (part d of Figure 3, right), it contacts four magnesium core basins and two ruthenium basins, reflecting a six-center interaction.

The distribution of the ELI-D attractors and the topology of their basins can be interpreted as a homoatomic partial structure of the three-bonded ruthenium atoms, which interact via multicenter bonds with the magnesium partial structure. Whereas the interaction between the ruthenium atoms can be described as a covalent one, the nature of the multicenter interactions and the role of both partial structures (cationic, anionic) cannot be understood in a straightforward way. Already applying the homolytic cleavage of the populations of all basins (i.e., covalent nonpolar bonding picture), one obtains the formal balance of $[Mg^{0.50+}]_3[Ru^{0.75-}]_2$, which suggests anionic character of the ruthenium substructure and fits the expectations, taking into account the electronegativity difference between magnesium and ruthenium. Assigning the whole populations of the multicenter bonds to the more electronegative ruthenium, that is, assuming a fully ionic bonding picture, one would obtain the balance $[Mg^{1.74+}]_3$-$[Ru^{2.61-}]_2$, which is quite unrealistic concerning the resulting electronic configuration of ruthenium but still showing the expected charge transfer.

An additional access to the nature of the interactions between the magnesium and ruthenium partial structures can be obtained by the estimation of the atomic charge according to the quantum theory of atoms in molecules (ref 22, QTAIM atoms). The zero-flux surfaces in the electron density within the unit cell of Mg_3Ru_2 define the shape and volume of QTAIM atoms of ruthenium and magnesium (Figure 4). Integration of the electron density within these shapes yields populations of 10.72 ($Mg^{1.28+}$) and 45.91 ($Ru^{1.91-}$) for magnesium and ruthenium, respectively. Thus, also the QTAIM representation confirms charge transfer from magnesium to ruthenium as expected from the electronegativity difference.

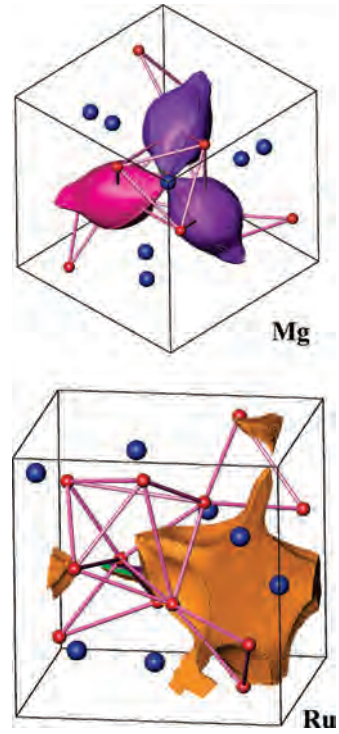

Figure 4. Shape of the QTAIM atoms of magnesium (top, 3 symmetrically equivalent atoms are shown) and ruthenium (bottom, one atom is shown) in the crystal structure of Mg_3Ru_2. Color coding as in Figure 3.

Conclusion

Crystal-structure refinement and analysis of chemical bonding in the compound Mg_3Ru_2 revealed existence of two 3D interpenetrating structural parts. Three-bonded ruthenium atoms interact to form a network by two-center bonds. This network interacts with the magnesium partial structure by means of four-, five-, and six-center bonds. The crystal-structure representation by means of the periodic nodal surface (part a of Figure 2) shows essential features of the bonding: (negatively charged) ruthenium network in one labyrinth, magnesium cations in another one, and multicenter interactions between the labyrinths. Different counting schemata result in the charge transfer from the magnesium substructure to the ruthenium one in agreement with the electronegativity difference between the components.

Acknowledgment. We thank H.-J. Göcke for the work at the scanning electron microscope and the Degussa-Hüls AG for a donation of ruthenium powder. This work was partially supported by the Deutsche Forschungsgemeinschaft.

Supporting Information Available: Crystallographic data in CIF format. This material is available free of charge via the Internet at http://pubs.acs.org.

IC800387A